arXiv:1402.6113v1 [cond-mat.mes-hall] 25 Feb 2014

Prediction of topological Nernst effect in silicene and similar 2D materials

I. Ahmed[1], M. Tahir[2], K. Sabeeh[1*]

[1]*Department of Physics, Quaid-i-Azam University, Islamabad 45320, Pakistan and*

[2]*Department of Physics, University of Sargodha, Pakistan*

Abstract

We consider Berry phase mediated Nernst effect in silicene. The low energy band structure of silicene consists of two valleys near the Dirac points, similar to graphene. The low energy transport properties of the quasiparticles can be described as Berry phase dependent phenomena. By contrast to graphene, silicene has strong spin-orbit interaction leading to opening of the gap in the energy spectrum and spin-splitting of the bands in each valley. If an electric field is applied perpendicular to the silicene sheet, it allows tunability of the gap. We show that this results in Berry-phase-supported spin and valley polarized Nernst effect when the system is subjected to a temperature gradient. The Nernst response can be used to create valley and spin polarization at the transverse edges of silicene sheet. The applied electric field also allows control of valley and spin polarization in silicene. The predicted valley and spin polarized Nernst effect in silicene is more general and applies to other two-dimensional (2D) buckled Dirac Fermion systems such as 2D germanium and tin.

Pacs:

I. INTRODUCTION

Silicene is a monolayer of silicon atoms[1], forming a buckled honeycomb structure [2, 3]. It does not occur naturally but it has been synthesized on metal surfaces[4, 5]. Its low energy band structure is similar to graphene with two inequivalent valleys at the Dirac points. By contrast to graphene, it has large Spin-Orbit Interaction (SOI) being more pronounced in silicon than in carbon[3], which induces a gap of 3.9meV, for graphene this gap is around 24μeV[6]. This significant SOI gives rise to two important phenomena. First, by opening the gap, it provides mass to the Dirac fermions[7, 8]. Second, it spin-splits the bands in each valley[7–9]. The latter property makes possible the manipulation of the spin degree of freedom, in addition to the valley degree of freedom, with possible applications in spintronics. Further, the gap in silicene is tunable by applying an external uniform electric field E_z perpendicular to the silicene sheet[7–11]. Interestingly, it has been shown that silicene shows a number of topologically protected phases, when subjected to the field E_z[7, 8, 11]. More importantly for this work, E_z-field breaks the Space Inversion (SI) symmetry of the system. Hence the Berry curvature is finite and sharply peaked at the two valleys. This gives rise to nontrivial topological electric transport phenomena. In graphene, it led to the prediction of valley Hall effect [12].

In this paper, we investigate the Berry phase effects on another class of transport coefficients, the thermoelectric transport coefficients. Our main focus is on topological Nernst effect. This Berry phase mediated Nernst effect exists independent of an external magnetic field. Prior to our work and relevant to it, there has been investigation of Nernst effect in gapped single and bilayer graphene[13] based on Berry phase formulation developed earlier[14, 15]. In both gapped graphene systems, the Nernst effect is valley dependent and can lead to valley polarization. By contrast in silicene, we will show that Nernst effect is valley as well as spin dependent. Therefore, in a generic Nernst measurement set up it can be used to generate valley as well as spin polarization which can have important technological implications.

The main question that we address, in this work, is the valley and spin tunability of the Nernst effect by an applied electric field. A related question is the ability to generate valley and spin polarization in silicene. These questions are important because silicene has rich physics, a variety of different phases[7, 8], and compatability with present silicon

microelectronics. Further, it has been recently shown that that the figure of merit which quantifies the thermoelectric effeciency of a material is much higher for silicene compared to graphene[23]. Therefore, it is believed, that silicene can be a better option for electrically tunable thermoelectric devices than graphene[10, 11].

II. BERRY CURVATURE AND MAGNETIC MOMENT

Silicene has a honeycomb structure of silicon atoms on sublattice sites A and B displaced from each other by a distance $2l$. The graphene-like low energy effective Hamiltonian of silicene, in the presence of SOI and subjected to a perpendicular E_z-field around Dirac point within each valley, can be expressed around the K_η point as[7, 8]

$$H_\eta^{s_z} = \hbar\upsilon\left(-\eta q_x\sigma_x + q_y\sigma_y\right) + \eta s_z\Delta_{so}\sigma_z + \Delta_z\sigma_z \tag{1}$$

where, $\eta = +/-$ for $K_{+,-}$ Dirac points (valley index), $\Delta_z = lE_z$, with l=0.23Å, $(\sigma_x, \sigma_y, \sigma_z)$ are Pauli matrices, υ is the Fermi velocity of Dirac fermions and (q_x, q_y) are the components of the wave vector relative to the Dirac point. The spin index $s_z = +/-$ for spin up $(\uparrow)$ and down $(\downarrow)$, respectively. In the absence of any $\widehat{s}_z$ nonconserving terms in the Hamiltonian, one can simply consider the two 2×2 subspaces corresponding to $s_z = \pm 1$ separately. The first term in the Hamiltonian, arises from nearest neighbour hopping and is the Dirac term, well known from studies in graphene. The second term is the intrinsic spin-orbit interaction term (Kane and Mele term) with spin-orbit gap of $\Delta_{so} = 3.9meV$. The third term is due to the uniform perpendicular electric field E_z with the electric field induced gap Δ_z. It generates a staggered sublattice potential between the sites A and B.

The Hamiltonian can be diagonalized analytically, and its energy spectrum is

$$\varepsilon_\eta^{s_z} = \pm\sqrt{\hbar^2\upsilon^2q^2 + \left(\Delta_z + \eta s_z\Delta_{so}\right)^2} \tag{2}$$

where +(-) solution is for electron(hole) bands. As we mentioned earlier, our model Hamiltonian Eq.(1) contains an external tunable parameter Δ_z, which can be tuned relative to Δ_{so}. So we have three possible situations: Δ_z is less than Δ_{so}, Δ_z is equal to Δ_{so} and Δ_z is greater than Δ_{so}. The energy dispersion, Eq. (2), for the three cases is presented in Fig.(1a), Fig.(1b) and Fig.(1c).

The eigenvectors for electron and hole states in K_+valley are $\left|\uparrow^e_{K+}\right\rangle = \begin{pmatrix} -\cos\frac{\theta}{2}e^{i\phi} \\ \sin\frac{\theta}{2} \end{pmatrix} \exp[iq_x x + iq_y y]$ and $\left|\uparrow^h_{K+}\right\rangle = \begin{pmatrix} \sin\frac{\theta}{2}e^{i\phi} \\ \cos\frac{\theta}{2} \end{pmatrix} \exp[iq_x x + iq_y y]$. $\theta = \tan^{-1}\frac{\hbar\upsilon q}{\Delta_z + \eta s_z \Delta_{so}}$ and $\varphi = \tan^{-1}\frac{q_y}{q_x}$ here. The states in K_- valley are time-reversed conjugates of the above states.

At this stage, it is necessary to discuss symmetry of our system because it dictates whether Berry curvature is finite and nonzero or not. This is important because topological transport will survive only when Berry curvature does not vanish at all points in the momentum space. Berry curvature is an odd function of q in the presence of Time-Reversal (TR) symmetry and an even function in the presence of Space Inversion (SI) symmetry[15, 16]. If both these symmetries are present, Berry curvature vanishes at all points in momentum space. The Δ_z term explicitely breaks SI symmetry, see Eq.(1)[12, 15, 16]. The TR symmetry when both the Dirac points is considered is intact. In this case, Berry curvature is finite and nontrivial which will have profound consequences for transport in the system. From the Hamiltonian, Eq. (1), and the eigenvectors, the Berry curvature for the conduction band (electrons), can be found:

$$\Omega^{s_z}_\eta = \left(\eta\frac{\hbar^2\upsilon^2}{2}\right)\frac{(\Delta_z + \eta s_z \Delta_{so})}{\left(\hbar^2\upsilon^2 q^2 + (\Delta_z + \eta s_z \Delta_{so})^2\right)^{\frac{3}{2}}}. \tag{3}$$

Note that Berry curvature has opposite signs in the two valleys for opposite spins as required by TR symmetry: $\Omega^+_+ = -\Omega^-_-$ and $\Omega^+_- = -\Omega^-_+$.

In an important study on valley contrasting physics in graphene[12], it was found that one of the properties that distinguishes valley degree of freedom is the magnetic moment. It is of orbital nature since SOI is weak in graphene. It depends on the valley index and can be used to create valley polarization in the presence of an external magnetic field. By contrast to graphene, SOI is relatively large in silicene. It spin splits the bands in silicene[7–9]. Therefore, in silicene, the Bloch fermions carry the spin magnetic moment in addition to the orbital magnetic moment which originates from the self rotation of their wave packet. It is important to note that valley magnetic moment in silicene has both valley and spin character. The orbital magnetic moment can be obtained from a semi-classical formulation of wave-packet dynamics and is given by[15, 17, 18]

$$\overrightarrow{m}\left(\overrightarrow{q}\right) = -i\left(\frac{e}{2\hbar}\right)\left\langle\overrightarrow{\nabla}_q u(q)\right| \times [H(q) - \varepsilon(q)]\left|\overrightarrow{\nabla}_q u(q)\right\rangle \tag{4}$$

where $|u(q)\rangle$ is the periodic part of the Bloch function, $H(q)$ is the Bloch Hamiltonian and $\varepsilon(q)$ is band dispersion. In analogy with graphene, since it depends on the valley index, it can be called the Valley Magnetic Moment (VMM). But we must remember that in silicene, unlike graphene, it is also a spin dependent quantity. For a 2D sheet the VMM is always normal to the plane. It comes out to be

$$m_{\eta}^{s_z} = \eta \left(\frac{e}{\hbar}\right) \left(\frac{\hbar^2 \upsilon^2}{2}\right) \frac{(\Delta_z + \eta s_z \Delta_{so})}{\left(\hbar^2 \upsilon^2 q^2 + (\Delta_z + \eta s_z \Delta_{so})^2\right)}. \tag{5}$$

It is concentrated at the Dirac points in the valleys. Furthermore, the VMM of the two valleys depends on the valley index. At the bottom of the band, where $q \to 0$, and for the parameters $\Delta_z = \Delta_{so} \sim 4$meV and $\upsilon \sim 5.5 \times 10^5$m/s, the VMM is about twice that of graphene (it is $63.78\mu_B$ for silicene whereas for graphene it is $30\mu_B$). This means, by contrast to graphene, we expect a stronger response in silicene to an applied perpendicular magnetic field. An applied magnetic field will couple to the valley magnetic moment. A net valley polarization, more moments in one valley compared to the other (population difference), will be achieved. The result is that an enhanced Pauli paramagnetism like phenomena with larger net magnetization is expected compared to graphene[12, 16]. Therefore, silicene is a better option to realize valley as well as spin polarization than graphene.

III. CHARGE VALLEY AND SPIN HALL CONDUCTIVITY

To determine the Nernst effect, we will proceed in two directions. First, we will determine the charge Hall conductivity and using the Mott relation arrive at the Nernst conductivity α_{xy}. This has the advantage that one can find an analytic expression for α_{xy}. The drawback is that the result is restricted to low temperature. The second approach is to employ the Berry formalism to compute the Nernst conductivity using the entropy density of the system. In this approach, one usually can not obtain analytic results at finite temperature because of the Fermi function integrals. At the end numerical integration is required.

Valley Hall Conductivity: We will begin with the first approach that requires calculating the charge Hall conductivity. This we can do by employing the Berry phase formalism. We are ignoring impurity scattering here and consider only the intrinsic contribution. In the presence of an in-plane electric field, fermions acquire anomalous velocity proportional to the Berry curvature that gives rise to the intrinsic Hall conductivity[18–20]. For a particular

valley (say K_+) and band n, the Valley Hall Conductivity (VHC) is given by

$$\sigma_{xy}^{v,n} = \frac{e^2}{\hbar}\int_0^{q_F}\frac{d^2q}{(2\pi)^2}\left[f_{\eta=+1,n}^{s_z=+1}(\varepsilon_q)\Omega_{\eta=+1}^{s_z=+1}(q) + f_{\eta=+1,n}^{s_z=-1}(\varepsilon_q)\Omega_{\eta=+1}^{s_z=-1}(q)\right] \tag{6}$$

where $f_{\eta,n}^{s_z}(\varepsilon_q)$ is the Fermi-Dirac distribution function for band n, spin s_z in valley η. In silicene, this depends on the valley index η, where $\eta = +1$ in the above equation, as well as the spin index s_z. The total valley Hall conductivity is the sum over all occupied bands for both valleys. We have determined the VHC, σ_{xy}^{v}, when the chemical potential μ is placed in the band gap, between the two spin split conduction bands (one band partially occupied) and above the bottom of both the conduction bands (both bands are partially occupied) for the following two cases: $\Delta_z < \Delta_{so}$ and $\Delta_z > \Delta_{so}$. The results, obtained from Eq.(6), are shown in the following table (1):

μ	$\Delta_z < \Delta_{so}$	$\Delta_z > \Delta_{so}$
in the band gap	0	$-\frac{e^2}{h}$
between spin split bands	$-\frac{e^2}{2h}\left[1-\frac{(\Delta_{so}-\Delta_z)}{\mu}\right]$	$-\frac{e^2}{2h}\left[1-\frac{(\Delta_{so}-\Delta_z)}{\mu}\right]$
above the bottom of both bands	$-\frac{e^2}{2h}\left(\frac{2\Delta_z}{\mu}\right)$	$-\frac{e^2}{2h}\left(\frac{2\Delta_z}{\mu}\right)$

These results highlight two important points. First, σ_{xy}^{v} for completely occupied bands has its maximum value $\frac{e^2}{2h}$, for partially filled bands it is unquantized. Second, it increases with E_z-field (or Δ_z) which allows tunability of σ_{xy}^{v}. We also need to discuss the situation when $\Delta_z = \Delta_{so}$. In this case, the system is gapless, the gap closes for spin-down bands, as shown in Fig. (1b). Eq. (3) suggests that for these bands, the Berry curvature vanishes and they do not contribute to σ_{xy}^{v}. The contribution comes from the spin-up bands. For a completely filled band σ_{xy}^{v} is $(\frac{e^2}{2h})$.

Spin Hall Conductivity: The Spin Hall Conductivity (SHC) for a single valley and band is

$$\sigma_{xy}^{s,n} = \frac{e^2}{\hbar}\int_0^{q_F}\frac{d^2q}{(2\pi)^2}\left[f_{\eta=+1,n}^{s_z=+1}(\varepsilon_q)\Omega_{\eta=+1}^{s_z=+1}(q) - f_{\eta=+1,n}^{s_z=-1}(\varepsilon_q)\Omega_{\eta=+1}^{s_z=-1}(q)\right] \tag{7}$$

The results, obtained from Eq.(7), are shown in the following table (2):

μ	$\Delta_z < \Delta_{so}$	$\Delta_z > \Delta_{so}$
band gap	$-\frac{e^2}{h}$	0
between spin splitted bands	$-\frac{e^2}{2h}\left[1+\frac{(\Delta_{so}-\Delta_z)}{\mu}\right]$	$-\frac{e^2}{2h}\left[1+\frac{(\Delta_{so}-\Delta_z)}{\mu}\right]$
above the bottom of both bands	$-\frac{e^2}{2h}\left(\frac{2\Delta_{so}}{\mu}\right)$	$-\frac{e^2}{2h}\left(\frac{2\Delta_{so}}{\mu}\right)$

σ^s_{xy} has its maximum value $\frac{e^2}{2h}$ for completely occupied bands and for partially occupied bands it is unquantized. Contrary to σ^v_{xy}, it decreases with increasing external E_z-field (or Δ_z). For $\Delta_z = \Delta_{so}$, similar to σ^v_{xy}, gapless bands do not contribute to σ^s_{xy}, where as a completely filled band contributes $\frac{e^2}{2h}$.

Hence, we find that Hall conductivities, σ^v_{xy} and σ^s_{xy}, are valley and spin dependent phenomena in silicene. Berry curvature has opposite sign in opposite valleys. An in-plane electric field will not only result in accumulation of charge from opposite valleys at opposite edges of the sample but also opposite spin.

IV. VALLEY AND SPIN NERNST EFFECTS

The quasiparticles in silicene carry energy in addition to charge. If silicene is subjected to a temperature gradient, current will flow transverse to the applied temperature gradient. This will happen even in the absence of an applied magnetic field. In this section, we calculate this spontaneous, Berry phase supported Nernst effect[14, 21, 22, 24]. We find that, in silicene, the Nernst effect is a valley and spin dependent phenomena. The expression for the current density is

$$j_x = \alpha_{xy} \left(- \bigtriangledown_y T \right) \tag{8}$$

where α_{xy} is the Nernst conductivity[14, 24]. It has been shown that α_{xy} is related to zero-temperature Hall conductivity through the Mott relation [14, 24]:

$$\alpha_{xy}(\varepsilon) = -\frac{1}{e} \int_0^\infty d\varepsilon \frac{\partial f}{\partial \varepsilon} \sigma_{xy}(\varepsilon) \frac{\varepsilon - \mu}{T} \tag{9}$$

where f is the Fermi-Dirac distribution function, μ is the chemical potential at zero-temperature (Fermi energy). α_{xy} comes out to be

$$\alpha_{xy} \simeq \frac{\pi^2 k_B^2 T}{3e} \left(\frac{d\sigma_{xy}(\mu)}{d\mu} \right). \tag{10}$$

As mentioned earler, in the Hamiltonian, Eq. (1), there is an external tunable parameter Δ_z. It has a direct impact on zero-temperature Hall conductivities, which in turn affect α_{xy}.

At higher temperatures, we will need to employ the second approach where it will be more convenient to calculate the coefficient $\overline{\alpha}_{xy}$ which determines the transverse heat current J^h in response to the electric field E : $J^h_x = \overline{\alpha}_{xy} E_y$. This is related to the Onsager relation

$\overline{\alpha}_{xy} = T\alpha_{xy}$[14, 19]. For a finite Berry curvature, the quasiparticles acquire an anomalous contribution and the coefficient of the transverse heat current. The valley Nernst conductivity is

$$\overline{\alpha}^{v}_{xy} = T\alpha_{xy} = \frac{e}{\beta\hbar}\sum_{\eta,s_z,n}\int \frac{d^2q}{(2\pi)^2}\Omega^{s_z}_{n,\eta}(q)s^{s_z}_{n,\eta}(q) \tag{11}$$

and the spin Nernst conductivity is

$$\overline{\alpha}^{s}_{xy} = T\alpha_{xy} = \frac{e}{\beta\hbar}\sum_{\eta,s_z,n}\int s_z\frac{d^2q}{(2\pi)^2}\Omega^{s_z}_{n,\eta}(q)S^{s_z}_{n,\eta}(q) \tag{12}$$

where $S^{s_z}_{n,\eta}(q) = -f^{s_z}_{n,\eta}(q)\ln f^{s_z}_{n,\eta}(q) - (1-f^{s_z}_{n,\eta}(q))\ln(1-f^{s_z}_{n,\eta}(q))$ is the entropy density of the Dirac fermion gas. $\Omega^{s_z}_{n,\eta}(q)$ and $f^{s_z}_{n,\eta}(q)$ are the Berry curvature and Fermi-Dirac distribution functions for Dirac fermions in valley η with spin $s_z = \pm 1$ in band n, respectively. For finite temperature, these expressions will have to be evaluated numerically.

Valley Nernst Effect: For a single valley we evaluated Eq. (11) numerically,the results are plotted in Fig.(2) and Fig.(3) at T=3K and 200K, respectively. First, we focus on low temperature results. In Fig.(2), Valley Nernst Conductivity (VNC) $\overline{\alpha}^{v}_{xy}$ is plotted versus chemical potential μ. As discussed earlier for completely occupied bands σ_{xy} is quantized in units of $\frac{e^2}{h}$ and for partially occupied bands it is unquantized. From Eq. (10), we find that completely filled bands do not contribute to $\overline{\alpha}^{v}_{xy}$, only partially filled bands contribute. In Figs.(2a) and (2c), there are two peaks. There is a single peak in Fig. (1b). Each peak corresponds to μ at the bottom of a partially filled band. In Figs.(2a) and (2c), first peak corresponds to lower band (spin-down band), where as the second peak corresponds to upper band (spin-up band). Whether the peak is positive or negative depends on the sign of the Berry curvature. First peak in Fig. (2a) is negative because the Berry curvature is negative for the contributing band . In Fig.(2b), we have a single peak, because only a single partially occupied band contributes to $\overline{\alpha}^{v}_{xy}$.

The low temperature results can be analyzed in light of Eq. (10) which is the central equation in the low temperature regime. α_{xy} is linear in temperature. It is proportional to the derivative of zero-temperature Hall conductivity σ_{xy} with respect to μ. In the band gap, σ_{xy} reaches its maximum value and it decreases on either side of band gap (as $1/\mu$)[15]. From table (1), it has opposite sign in conduction and valence bands. Therefore, α_{xy} is discontinuous and with a peak as μ touches the bottom of a band and Eq. (10) shows that

it decreases as $1/\mu^2$[13]. The magnitude of each peak depends on the Berry curvature of respective band.

In Fig. (3), $\overline{\alpha}^v_{xy}$ is plotted in the high temperature regime. In this regime, peaks in $\overline{\alpha}^v_{xy}$ are completely lost. This is due to the large contribution from thermal excitations. This occurs when $k_B T \tilde{} \ \Delta_{so}$.

Spin Nernst Effect: In this part we are going to discuss behaviour of spin Nernst conductivity $\overline{\alpha}^s_{xy}$. We have evaluated Eq. (12) numerically and the results are plotted in Figs.(4a,4b,4c) at T=3K, our focus is on the low temperature regime. Spin Nernst conductivity has been evaluated as a function of the chemical potential as Δ_z is varied relative to Δ_{so}. Each partially occupied band contributes a peak to $\overline{\alpha}^s_{xy}$ whose magnitude and direction depends on the magnitude and direction of the respective band's Berry curvature. Its behavior follows that of σ^v_{xy} and α_{xy}: $\overline{\alpha}^s_{xy}$ is proportional to $1/\mu$, seen in table 2, and Eq: (10) shows that $\overline{\alpha}^s_{xy}$ is proportional to $1/\mu^2$. While discussing the behaviour of $\overline{\alpha}^s_{xy}$, it is important to discuss a situation where both spin-up and spin-down Nernst conductivities overlap. For a particular μ, in each case, either spin-up or spin-down contribution dominates. Hence, we can obtain finite spin-polarized conductivity by tuning the two relevant parameters: chemical potential μ and Δ_z through the applied electric field.

Experimental Realization: Magnetothermoelectric measurement techniques for 2D systems are well established and have been successfully employed to investigate the intriguing properties of Dirac Fermion systems like graphene[25–27]. Furthermore, Nernst effect has also been studied in systems with magnetic order such as ferromagnetic semiconductors[21, 28]. Along the same lines, it is quite feasible to carry out Nernst effect studies in silicene proposed in this work.

The valley and spin-polarized Nernst effect predicted for silicene is more general and applies to similar low buckled 2D Dirac Fermion systems of group IVA elements such as germanium (germanene) and tin[3, 10, 11, 29]. In this regard, we note that the Hamiltonian in Eq.(1) can also be used to describe germanene, which is a honeycomb structure of germanium. Here, the SOI is even stronger (43 meV) with $l = 0.33\mathring{A}$ and the analysis presented for silicene is also valid for germanene.

V. SUMMARY

We have investigated Nernst Hall conductivity in silicene in the presence of a uniform electric field perpendicular to the silicene sheet. The electric field allows tunability of the band gap in silicene. Due to the relatively strong spin-orbit interaction, Nernst Hall conductivity is both valley and spin-dependent. This is in contrast to graphene. We have employed Berry phase formalism to detremine the Nernst effect. We show that it is possible to generate spin as well as valley polarization in silicene. By varying the electric field strenth relative to the spin-orbit interaction strength we can control valley and spin polarization in silicene.

VI. ACKNOWLEDGEMENT

K. Sabeeh would like to acknowledge the support of the Abdus Salam International Center for Theoretical Physics (ICTP) in Trieste, Italy through the Associate scheme where a part of this work was completed. I. Ahmed and K. Sabeeh further acknowledge the support of Higher Education Commission (HEC) of Pakistan through project No. 20-1484/R&D/09. The authors gratefully acknowledge enlightening discussions with Sumanta Tewari, Markus Mueller and Di Xiao during the completion of this work.

*Corresponding Author: ksabeeh@qau.edu.pk

---

[1] K. Takeda and K. Shiraishi, Phys. Rev. B 50,14916 (1994).

[2] G. G. Guzman-Verri and L. C. Lew Yan Voon, Phys. Rev. B 76, 075131 (2007)

[3] C.-C. Liu, W. Feng and Y. Yao, Phys. Rev. Lett. 107, 076802 (2011).

[4] P. Vogt, P. D. Padova, C. Quaresima, J. Avila, E. Frantzeskakis, M. C. Asensio, A. Resta, B. Ealet, and G. L. Lay, Phys. Rev. Lett. 108, 155501 (2012).

[5] B. Lalmi, H. Oughaddou, H. Enriquez, A. Kara, S. Vizzini, B. Ealet, and B. Aufray, Appl. Phys. Lett. 97, 223109 (2010).

[6] D. Kochan, M. Gmitra, and J. Fabian, Conf. Vol. 8461, Spintronics V, 84610L (2012).

[7] Motohiko Ezawa, Phys. Rev. B 87, 155415 (2013).

[8] Motohiko Ezawa, Phys. Rev. Lett. 109, 055502 (2012).

[9] M. Tahir, A. Manchon, K. Sabeeh and U. Schwingenschlogl, Appl. Phys. Lett. 102, 162412 (2013).

[10] N. D. Drummond, V. Zólyomi, and V. I. Fal'ko, Phys. Rev. B 85, 075423 (2012).

[11] Motohiko Ezawa, New J. Phys. 14, 033003(2012).

[12] D. Xiao, W. Yao and Q. Niu, Phys. Rev. Lett. 99, 236809 (2007).

[13] C. Zhang, S. Tewari and S. Das Sarma, Phys. Rev. B 79, 245424 (2009).

[14] D. Xiao, Y. Yao, Z. Fang and Q. Niu, Phys. Rev. Lett. 97, 026603 (2006).

[15] D. Xiao, M.-C. Chang, Q. Niu, Rev. Mod. Phys. 82, 1959 (2010).

[16] Di Xiao, Ph.D. Dissertation, The University of Texas, Austin, 2007.

[17] J. Shi, G. Vignale, D. Xiao and Q. Niu, Phys. Rev. Lett. 99, 197202 (2007).

[18] M.-C. Chang and Q. Niu, Phys. Rev. B 53, 7010 (1996).

[19] N. R. Cooper, B. I. Halperin and I. M. Ruzin, Phys. Rev. B 55, 2344 (1997).

[20] T. Jungwirth, Q. Niu, and A. H. MacDonald, Phys. Rev. Lett. 88, 207208 (2002).

[21] W.-L. Lee, S. Watauchi, V. L. Miller, R. J. Cava and N. P. Ong, Phys. Rev. Lett. 93, 226601 (2004).

[22] N. P. Ong and W.-L. Lee, arXiv: 0508236, Proceedings of ISQM-Tokyo (2005).

[23] K. Yang *et.al.*, arXiv: 1310.0971 (2013).

[24] C.-P. Chuu, M.-C. Chang and Q. Niu, Solid State Comm,150, 533 (2010).

[25] J. G. Checkelsky and N. P. Ong, Phys. Rev. B 80, 081413(R) (2009).

[26] P. Wei, W. Bao, Y. Pu, C. N. Lau, and J. Shi, Phys. Rev. Lett. 102, 166808 (2009).

[27] Y. M. Zuev, W. Chang, and P. Kim, Phys. Rev. Lett. 102, 096807 (2009).

[28] C. M. Jaworski, et al., Nature Materials 9, 898 (2010).

[29] C. C. Liu, H. Jiang, and Y. Yao, Phys. Rev. B 84, 195430 (2011).

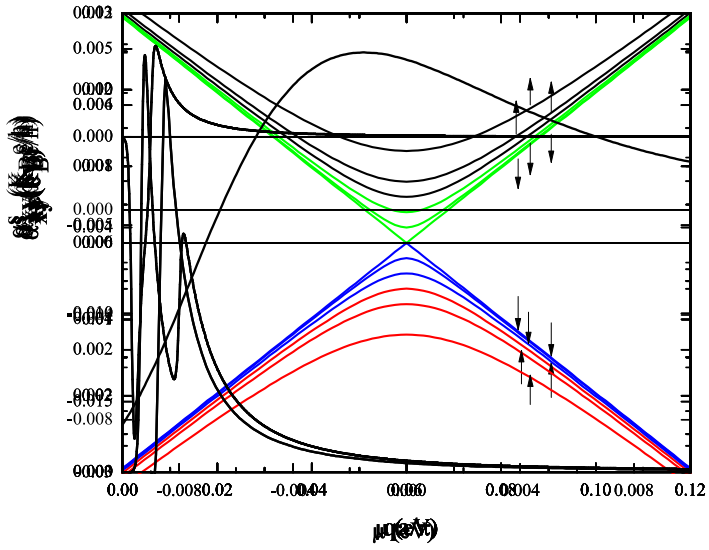

Fig
$\Delta_z =$ meV